THE JOURNAL OF PHYSICAL CHEMISTRY B

Article

pubs.acs.org/JPCB

Probing the Sources of the Apparent Irreproducibility of Amyloid Formation: Drastic Changes in Kinetics and a Switch in Mechanism Due to Micellelike Oligomer Formation at Critical Concentrations of IAPP

Jeffrey R. Brender,[†] Janarthanan Krishnamoorthy,[†] Michele F. M. Sciacca,[†,‡] Subramanian Vivekanandan,[†] Luisa D'Urso,[‡] Jennifer Chen,[†] Carmelo La Rosa,[‡] and Ayyalusamy Ramamoorthy*[,†]

[†]Biophysics, University of Michigan, Ann Arbor, Michigan 48109-1055, United States

[‡]Department of Chemical Sciences, University of Catania, Catania, Italy

Supporting Information

ABSTRACT: The aggregation of amyloidogenic proteins is infamous for being highly chaotic, with small variations in conditions sometimes leading to large changes in aggregation rates. Using the amyloidogenic protein IAPP (islet amyloid polypeptide protein, also known as amylin) as an example, we show that a part of this phenomenon may be related to the formation of micellelike oligomers at specific critical concentrations and temperatures. We show that pyrene fluorescence can sensitively detect micellelike oligomer formation by IAPP and discriminate between micellelike oligomers from fibers and monomers, making pyrene one of the few chemical probes specific to a prefibrillar oligomer. We further show that oligomers of this type reversibly form at critical concentrations in the low micromolar range and at specific critical temperatures. Micellelike oligomer formation has several consequences for amyloid formation by IAPP. First, the kinetics of fiber formation increase substantially as the critical concentration is approached but are nearly independent of concentration below it, suggesting a direct role for the oligomers in fiber formation. Second, the critical concentration is strongly correlated with the propensity to form amyloid: higher critical concentrations are observed for both IAPP variants with lower amyloidogenicity and for native IAPP at acidic pH in which aggregation is greatly slowed. Furthermore, using the DEST NMR technique, we show that the pathway of amyloid formation switches as the critical point is approached, with self-interactions primarily near the N-terminus below the critical temperature and near the central region above the critical temperature, reconciling two apparently conflicting views of the initiation of IAPP aggregation.

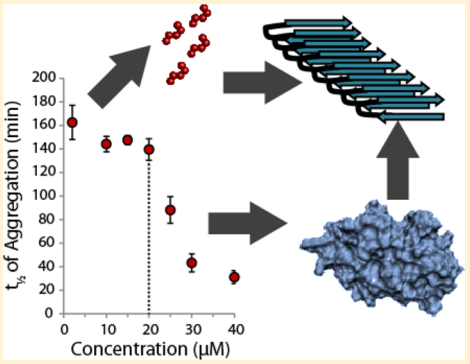

INTRODUCTION

Inappropriate, uncontrolled protein aggregation is emerging as a common thread linking many types of common pathologies, including some very common and currently incurable disorders.[1] The most widespread type of aggregation is the irreversible conversion of monomeric proteins into long fibers with a characteristic β-sheet structure known as amyloids.[2,3] Because of the purported involvement of amyloidogenic proteins of this type in Alzheimer's and other very serious neurodegenerative disorders, considerable effort has been made to understand the process of amyloid formation with the intent of developing approaches to stop it.[4,5]

Unfortunately, progress in this area has been partially stymied by the seeming irreproducibility of many results.[6−8] There have been several recent high-profile examples where an apparent success has been replicated with mixed outcomes.[9−14] The use of controlled in vitro conditions allows certain questions to be answered in a more precise manner.[8] However, even under controlled in vitro conditions a consensus is lacking for many amyloidogenic proteins on the specific mechanisms involved in amyloid formation.[15−17] The lack of consensus on mechanism and the complex nature of the various species along the aggregation pathway have proven frustrating for drug development, as many such drugs seek to target specific oligomers along the aggregation pathway.[5,18,19] Part of the lack of consensus appears to stem from the sensitivity of both the kinetics and mechanism to apparently minor changes in environmental conditions. Even minor changes, such as a buffer substitution,[20,21] can lead to substantial changes in pathway and intermediates. However, while early reports suggested that amyloid formation may be truly random, controlled by the stochastic generation of an extremely limited number of seeding nuclei,[6] later research has shown that the apparent irreproducibility of many amyloids can be tamed by a

Received: November 24, 2014
Revised: January 16, 2015

DOI: 10.1021/jp511758w
J. Phys. Chem. B XXXX, XXX, XXX−XXX

careful consideration of starting conditions and knowledge of the factors influencing aggregation.[7,22−25] Using amyloidogenic peptide IAPP as a model system, we show that relatively small changes in concentration and temperature can cause large but reproducible changes in both the rate and mechanism of aggregation through the reversible formation of specific types of oligomers.

MATERIALS AND METHODS

See the Supporting Information for detailed experimental procedures.

RESULTS

Rate of Fiber Formation by IAPP Is Nearly Independent of Concentration below a Threshold Concentration. To gain insight into some of the factors that may cause such sensitivity to environmental conditions, we first looked at the concentration dependence of amyloid formation in model amyloid protein IAPP by using amyloid-specific dye thioflavin T (ThT). Islet amyloid polypeptide (IAPP, sequence KCNTATCATQRLANFLVHSSNNFGAILSSTNVGSNTY-NH_2 with an amidated C-terminus and a disulfide bridge between residues 2 and 7) is a peptide hormone whose pathological aggregation has been implicated in the development of type II diabetes.[26] IAPP is also frequently used as a model for amyloid formation from natively unstructured proteins, an important class of amyloidogenic proteins that also includes Aβ (implicated in Alzheimer's disease) and α-synuclein (Parkinson's).[27]

The results of the ThT assay are shown in Figure 1 with the time to half completion of fiber formation ($t_{1/2}$) plotted on the

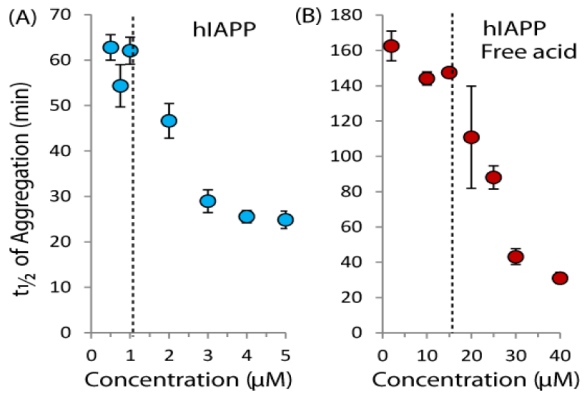

Figure 1. The rate of amyloid formation of hIAPP increases sharply near a threshold concentration. Time to one-half completion of amyloid formation as a function of hIAPP concentration for the native amidated hIAPP sequence (A) and the free acid version (B) as measured by amyloid-specific dye ThT at 25 °C with orbital shaking (pH 7.3 10 mM sodium phosphate buffer, 100 mM NaCl). The dashed lines indicate the approximate threshold concentrations from the aggregation experiment. Error bars represent SEM for six (hIAPP) or three (hIAPP free acid) experiments.

y axis. The full time courses for the ThT assay can be found as Figure S1 in the Supporting Information. For these experiments, two different forms of IAPP were used, the native human peptide which is amidated at the C-terminus (hIAPP) and the free acid form of the peptide (hIAPP free acid) which is known to aggregate slower than the native peptide.[28] The reason for this difference between the free acid and amidated forms is currently unclear but may be related either to an increase in electrostatic repulsion in the free acid form,[29] the folding of the C-terminus against His18 in the free acid form,[29,30] or to a difference in the rigidity of the C-terminus between the free acid and amidated forms of hIAPP.[31,32] All three measures of fiber formation kinetics reveal an unusual feature for both peptides: fiber formation is nearly independent of peptide concentration below a specific concentration, which we define as a "threshold concentration" for aggregation (~1 μM for hIAPP and 15 μM for the hIAPP free acid in this experiment, shown as dashed lines in Figure 1).

Rate of Fiber Formation by IAPP Increases Sharply at a Threshold Concentration. Another look at the ThT kinetics reveals an even more striking feature. While fiber formation is nearly independent of concentration at low concentrations, the rate of fiber formation sharply increases at the threshold concentration. The sharp changes apparent at the threshold concentration are unexpected, as most (but not all)[33−36] current theories of amyloid formation predict a power law dependence of the fibrillization rate on the initial concentration.[35] In particular, the nucleation-dependent polymerization theory commonly used to model amyloid formation predicts that the rate-determining step is the buildup of an energetically unfavorable nucleus of size n during the lag phase.[37] After this buildup, aggregation proceeds quickly, leading to the characteristic sigmoidal shape of the kinetics of most amyloidogenic proteins. If IAPP aggregation follows such a mechanism, then the concentration dependence of $t_{1/2}$ should follow the power law distribution αc^{β} where the exponent β is dependent on the nucleus size.[35,38] This power law relationship should translate to a smooth decrease in the aggregation time $t_{1/2}$ with increasing concentrations of hIAPP. While this power law relationship is roughly apparent above the threshold concentration (Figure S2), near the threshold concentration the kinetics sharply deviate from the expected values. This deviation suggests that some other mechanism affects aggregation that is not accounted for in the traditional nucleation-dependent polymerization model and is explored in more detail below.

Micellelike hIAPP Oligomers Form near a Critical Micellar Concentration That Can Be Detected Sensitively and Specifically by Pyrene Fluorescence. Specifically, the existence of a threshold concentration is reminiscent of micelle formation. Micellelike oligomers have been suggested to be intermediates along the aggregation pathway of Aβ,[33,34,39] another amyloidogenic peptide that shares many properties with hIAPP.[33,34,40] For IAPP specifically, a short fragment of hIAPP free acid ($hIAPP_{20-29}$) has been proven to form micelles,[41] and micelle formation by full-length hIAPP has been theoretically predicted based on kinetic modeling.[42,43] In particular, the formation of off-pathway micelles or other aggregates has been proposed to explain the apparent concentration independence of hIAPP aggregation.[41,43,44] The low concentrations involved (most previous measurements have used in excess of 5 μM hIAPP) made directly detecting concentration-dependent self-association by dynamic light scattering difficult. Instead, we employed pyrene fluorescence experiments to probe the formation of hydrophobic clusters by peptide self-association at a series of concentrations. The fluorescence emission spectrum of pyrene is environmentally sensitive to the ratio of the fluorescence intensities of the first (I_I) and third (I_{III}) vibronic bands decreasing as the hydrophobicity of the environment increases (Figure 2A).[45]

DOI: 10.1021/jp511758w
J. Phys. Chem. B XXXX, XXX, XXX−XXX

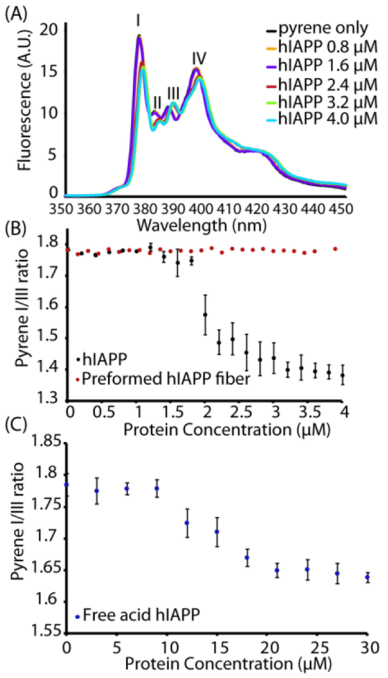

Figure 2. Pyrene specifically detects concentration-dependent oligomer formation over amyloid fibers. (A) Fluorescence emission spectra of 1 μM pyrene with the indicated concentrations of hIAPP upon excitation at 334 nm. (B) Plots of the pyrene I_I/I_{III} ratio measured during a titration with freshly dissolved hIAPP at pH 7.3 (black circles) or preformed fibers of hIAPP (allowed to aggregate beforehand for 24 h at 37 °C with shaking, red circles). (C) Corresponding plots of the pyrene I_I/I_{III} ratio measured with hIAPP free acid. Note the difference in the *x*-axis scale from that in (B). All measurements were performed in a solution of 20 mM phosphate buffer, 50 mM NaCl, and 1 μM pyrene at 25 °C. Errors bars indicate SEM (measurement preformed in triplicate).

In particular, a decrease in the first band intensity and an increase in the third band indicate the formation of a micellelike structure. By analogy to previous experiments on detergent micelles, an apparent CMC where the disordered monomer aggregates to form a micelle with a hydrophobic interior can therefore be defined by the inflection point in a plot of this ratio as a function of protein concentration.[40,46]

Both hIAPP and hIAPP free acid solutions show a sharp reduction in the I_I/I_{III} ratio as a threshold concentration is approached. hIAPP at pH 7.4 shows this this apparent CMC is near 2 μM (Figure 2B black circles, the full pyrene spectrum is shown in Figure 2A), which is close to the apparent critical micellar concentration (CMC) of the $hIAPP_{20-29}$ fragment obtained by other means[41] (3.5 μM) and close to theoretical predictions for the CMC of hIAPP itself based on kinetic modeling (~1.3−1.5 μM).[42,43] A similar experiment performed using the free acid form of hIAPP (Figure 2C) gives a higher threshold concentration of ~15 μM. Notably, the pyrene emission experiment is sensitive only to the formation of micellar oligomeric species of hIAPP. No change in the I_I/I_{III} band intensity ratio was observed by titrating the pyrene solution with preformed fibers of hIAPP (Figure 2B, red circles), which suggests that pyrene has the rare property among chemical probes of being almost completely selective for nonfibrillar oligomer forms over amyloid fibers.[47]

Micellelike Oligomer Formation Is Reversible with Changes in Concentration and Temperature. Micelles formed from detergents and other amphiphilic compounds are usually dynamic structures with rapid exchange occurring between the micelle and monomer subunits in solution. Because of this rapid exchange between the monomer and micelle, dilution beyond the CMC usually results in the immediate dissociation of the micelle. For some micelles, critical solution temperatures also exist which control the formation of the micelle; micelles do not form above the upper critical solution temperature or below the lower critical solution temperature.[48] The dynamic nature of micelles is in marked contrast from the high kinetic stability of amyloid fibers and many types of oligomeric proteins. For example, stable populations of certain types of oligomers can be isolated by size exclusion chromatography,[49] a feat that would be difficult[50,51] if equilibrium was rapidly re-established as it is for micellar-type aggregates.

We first tested the reversibility of the formation of hIAPP micellar oligomers by diluting a sample of hIAPP above the threshold concentration and comparing the pyrene I_I/I_{III} ratio to that obtained by titrating in hIAPP. If the oligomer can rapidly dissociate like a micelle, then the dilution and titration curves should be identical. On the other hand, if the oligomers are kinetically stable like amyloid protofibers, then the I_I/I_{III} ratio will not decrease as the sample is diluted. When a 4 μM sample of hIAPP is progressively diluted, the pyrene I_I/I_{III} ratios obtained by titration and dilution closely match (Figure 3), indicating that the formation of micellelike oligomer hIAPP is a reversible process.

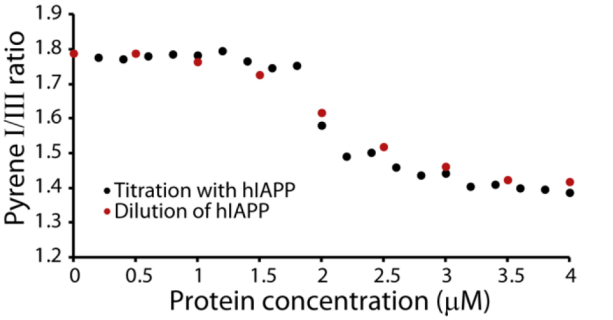

Figure 3. Concentration-dependent oligomer formation of hIAPP is reversible. Plots of the pyrene I_I/I_{III} ratio measured either by titration with freshly dissolved hIAPP at pH 7.3 (black circles) or by dilution from 4 μM hIAPP (red circles). All measurements were performed in a solution of 20 mM phosphate buffer and 50 mM NaCl at 25 °C. The pyrene concentration is kept constant at 1 μM for all experiments.

We next sought to determine if a critical temperature for micellelike oligomer formation exists by fixing the concentration of hIAPP above the threshold concentration at 4 μM and measuring the pyrene I_I/I_{III} ratio as a function of temperature (Figure 4) at pH 7.3. The plot clearly indicates that the formation of micellelike oligomers does not occur at temperature below 10 °C, indicating that sample concentration by itself is not sufficient to induce oligomer formation. The I_I/I_{III} ratio of pyrene in the absence of hIAPP did not change with temperature, confirming that the fluorescence change is the result of oligomer formation and not temperature-dependent changes in fluorescence. For further confirmation, we checked the temperature dependence of the peak intensity in the ^{15}N-SOFAST HMQC spectra of hIAPP free acid (Figure 5), as it is expected that oligomer formation will lead to a decrease in intensity either due to the creation of NMR-invisible oligomers

DOI: 10.1021/jp511758w
J. Phys. Chem. B XXXX, XXX, XXX−XXX

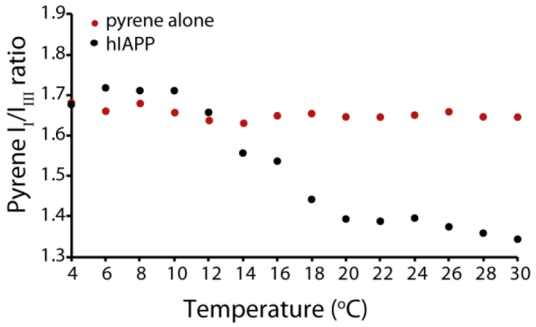

Figure 4. Oligomer formation of hIAPP occurs only above an apparent critical solution temperature. Plot of the pyrene I_I/I_{III} ratio in the presence of 4 μM hIAPP at pH 7.3 at increasing temperature values (black circles). As a control, the pyrene I_I/I_{III} ratio in the absence of hIAPP was collected (red circles). All measurements were performed at pH 7.3 in a solution of 20 mM phosphate buffer, 50 mM NaCl, and 1 μM pyrene.

at the expense of NMR-visible monomers or due to line broadening from conformational exchange. At pH 5, where no oligomers were detected by pyrene, the intensity increases with temperature in the ^{15}N-SOFAST HMQC spectra, as is typically observed with many disordered peptides and proteins.[52] By contrast, at pH 7.3 the intensity drops abruptly at 10 °C, identical to the pyrene results. Decreasing the temperature from 30 to 4 °C almost entirely reverses the intensity changes (Figure S3), strongly indicating that oligomer formation is reversible with temperature as well as concentration.

Apparent CMC for Oligomer Formation Correlates with Amyloidogenic Propensity. When the ThT aggregation assay results (Figure 1) are compared to the pyrene fluorescence results, it can be seen that $t_{1/2}$ clearly clusters into two regimes, with the dividing line near the CMC as determined by the pyrene fluorescence assay. Below the CMC, $t_{1/2}$ is nearly independent of concentration. At the CMC, $t_{1/2}$ declines sharply as the concentration is increased. This particular type of concentration dependence suggests that two separate mechanisms of aggregation are operational above and below the apparent CMC value.

A comparison of Figures 1 and 2 also reveals a possible relationship between the threshold concentration and the amyloidogenic propensity. The free acid form of hIAPP has a higher CMC than hIAPP (~15 μM vs ~1.5 μM). Interestingly, the ThT experiments also show that aggregation of the free acid form of hIAPP is significantly slower below the CMC than for hIAPP, but the rates of both peptides are similar above the CMC.

We further explored this correlation between the aggregation rate and threshold concentration for oligomer formation by using variants of IAPP with significantly slower aggregation rates and pH ranges in which aggregation is significantly slowed. The rat variant of IAPP (rIAPP, sequence KCNTATCATQRLANFLV**R**SSNN**L**G**PV**L**PP**TNVGSNTY-NH_2; residues different from those of hIAPP are in bold) is normally nonamyloidogenic and nontoxic to cells.[53,54] As expected, rIAPP did not form oligomers over the concentration range tested (Figure 6, green circles). Similarly, the N-terminal 1−19

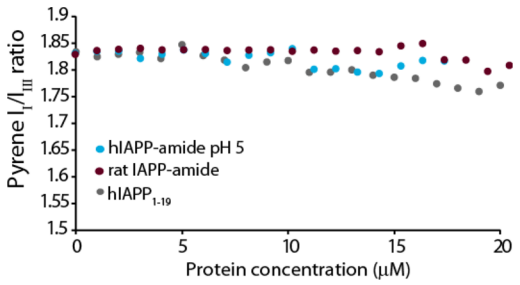

Figure 6. Non- or weakly amyloidogenic IAPP variants do not form pyrene-detectable oligomers. Plots of the pyrene I_I/I_{III} ratio measured during a titration with freshly dissolved hIAPP at pH 5 (cyan circles), nonamyloidogenic amidated rat IAPP (maroon circles), or weakly amyloidogenic $hIAPP_{1-19}$ (gray circles). All measurements were performed in a solution of 20 mM phosphate buffer, 50 mM NaCl, and 1 μM pyrene at 25 °C.

fragment of hIAPP ($hIAPP_{1-19}$) is significantly less amyloidogenic than the full-length peptide. While the 1−19 region of hIAPP is believed to be involved in peptide self-association, $hIAPP_{1-19}$ itself forms amyloid slowly and only at high (mM) concentrations.[55] Like rIAPP, $hIAPP_{1-19}$ did not form oligomers over the concentration range tested (Figure 6). Finally, we tested for possible oligomer formation of hIAPP at pH 5. At this pH, His18 is protonated, and it has been observed by multiple groups that fiber formation is significantly slower at pH 5 than at pH 7.3. Like the less-amyloidogenic $hIAPP_{1-19}$ and rIAPP variants at pH 7.3, micellelike oligomers of hIAPP did not form at pH 5 over the concentration range tested (Figure 6, green circles)

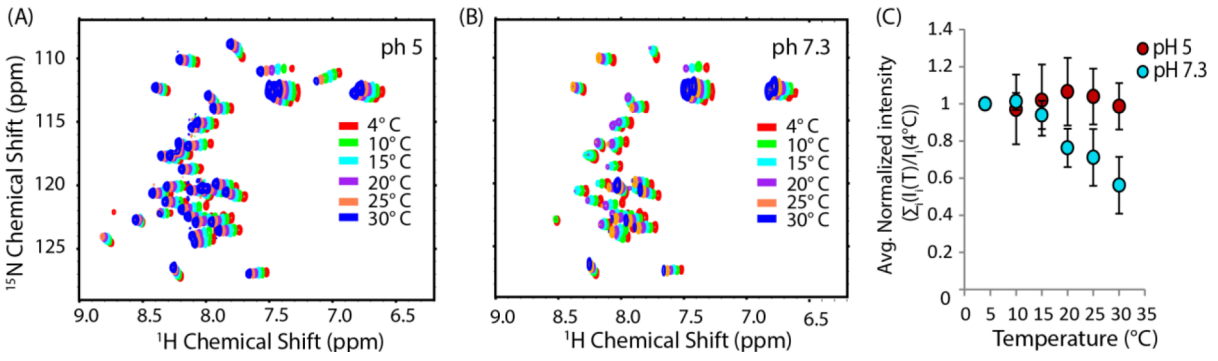

Figure 5. Peak intensity in the NMR spectra of the hIAPP free acid sharply decreases at a critical temperature at pH 7.3 but not pH 5. Temperature dependence of the ^{15}N HSQC spectra of 78 μM hIAPP free acid in a solution of 20 mM sodium phosphate buffer and 50 mM NaCl at pH 5 (A) and pH 7.3 (B). (C) Average of the peak intensity relative to the value at 4 °C as a function of temperature. Error bars represent the SEM, where N is considered to be the number of residues.

DOI: 10.1021/jp511758w
J. Phys. Chem. B XXXX, XXX, XXX−XXX

IAPP Forms Distinctly Different Oligomers above and below the Critical Temperature and Concentration. The existence of separate fast and slow regimes suggests that aggregation may proceed by a different mechanism above and below the critical concentration and temperature. To gain atomic-level insight into the process of oligomer formation, we first acquired ^{1}H NMR spectra of the free acid form of hIAPP above (40 μM) and below (10 μM) the apparent CMC from the pyrene experiments at 37 °C and pH 7.3 (Figure 7).

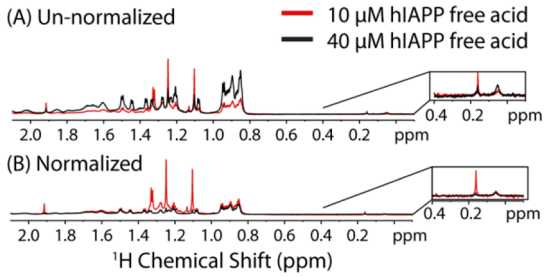

Figure 7. Dilution changes the ^{1}H NMR spectra of hIAPP free acid. ^{1}H NMR spectra of 10 and 40 μM hIAPP free acid at 37 °C in a solution of 20 mM sodium phosphate buffer and 50 mM NaCl at pH 7.3 normalized to the number of scans only (A) and normalized to both the concentration and number of scans (B). Inset: Strongly shielded peaks previously correlated with oligomer formation.

Differences in the normalized spectra are immediately apparent. First, the average intensity is higher at 10 μM than at 40 μM once both spectra are normalized for concentration (Figure 7B). Since the signal from slowly tumbling large oligomers would be broadened beyond detection, the increase in intensity upon dilution is consistent with the formation of large oligomers that are immediately dissociated upon dilution, consistent with the pyrene fluorescence results. Furthermore, the increase in intensity upon dilution is not uniform. Instead, the largest overall changes are in the aliphatic region of the spectrum, consistent with the involvement of the side chains of hydrophobic residues in micellelike oligomer formation. In particular, several peaks in this region are noticeably narrower, more intense, or shifted in frequency in the low-concentration spectra. This finding is consistent with micellelike oligomer formation, as hydrophobic side chains facing the interior of the micelle are expected to be more strongly perturbed than the hydrophilic side chains facing the outside. It is important to note that all NMR experiments were performed in Shigemi tubes, which lack a bulk air−water interface, indicating that a bulk air−water interface is apparently not essential for either concentration- or temperature-dependent oligomer formation.

It has been shown previously for a variety of amyloidogenic proteins[56−59] including hIAPP[60] that strongly shielded, broad peaks in the region of 0.2 to −1 ppm correspond to the mobile side chains in an oligomeric complex (Figure 7 inset). Interestingly, at pH 7.3 but below the CMC, an additional peak can be seen in this region at 0.16 ppm that disappears as the concentration is increased. This finding suggests that another type of oligomer may be present at pH 7.3 at low concentration that is unobservable as the concentration is raised.

While the NMR results suggest that an additional oligomer not detected by pyrene may form at low concentrations of IAPP at pH 7.3 but not pH 5, the results are not conclusive because this peak may reflect only collapsed states of the IAPP monomer,[60] differences in hydrogen exchange rates, and other factors. To more directly probe the existence of other types of oligomers, we directly visualized the aggregates formed during incubation above (25 °C) and below (4 °C) the critical temperature using AFM (Figure 8). In this experiment, IAPP is

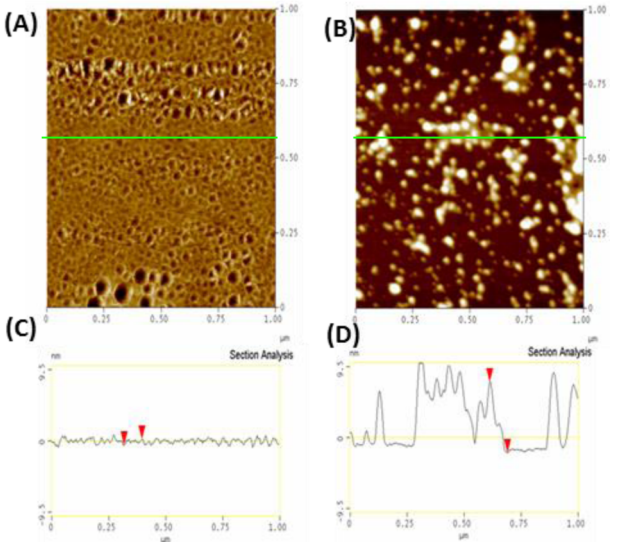

Figure 8. hIAPP forms a different type of oligomer following brief incubation at 4 or 25 °C. Top: Different aliquots of the same solution of 10 μM hIAPP (initially at 4 °C, 10 mM phosphate buffer, 100 mM NaCl, pH 7.4) were either left at 4 °C (A) or heated to 25 °C (B) and then quickly deposited on SiO_2, frozen with liquid N_2, and lyophilized to preserve the morphology of the original aggregates and those obtained via tapping-mode AFM in air (40% humidity). Bottom: Section analysis of samples initially prepared at 4 °C (C) and 25 °C (D) showing the height distribution along the green lines in (A) and (B).

first dissolved at pH 5 at either 25 °C or below 4 °C before the pH is quickly adjusted to 7.3 and the sample is immediately deposited on mica. At 25 °C, a large population of approximately spherical oligomers of approximately 12−15 nm radius along with another population of elongated oligomers are apparent immediately after incubation (Figure 8B,D). Oligomers of this type were not present when the sample was incubated at 4 °C. Instead, a close inspection of the high-resolution AFM images of hIAPP incubated at 4 °C show a smaller population of a different type of oligomer, disclike in shape with a height of approximately 1 nm but with a similar diameter to that of the 25 °C oligomers (Figure 8A,C). We therefore conclude that at least two distinct populations of oligomers likely exist above the critical temperature and threshold concentration, one of which is not detectable below either limit.

IAPP Self-Association Is Primarily at the N-Terminus below the Critical Temperature and in the Central Amyloidogenic Region above the Critical Temperature. The existence of distinct types of oligomers above and below the critical concentration and temperature suggests different interactions and possibly different mechanisms involved in fiber formation. We tested this possibility by probing the interactions of the monomer with the oligomer by dark exchange saturation transfer (DEST) NMR experiments.[61−63] In the DEST experiment (and related off-resonance[64] and saturation transfer experiments[65−69]), the line broadening in the monomer

DOI: 10.1021/jp511758w
J. Phys. Chem. B XXXX, XXX, XXX−XXX

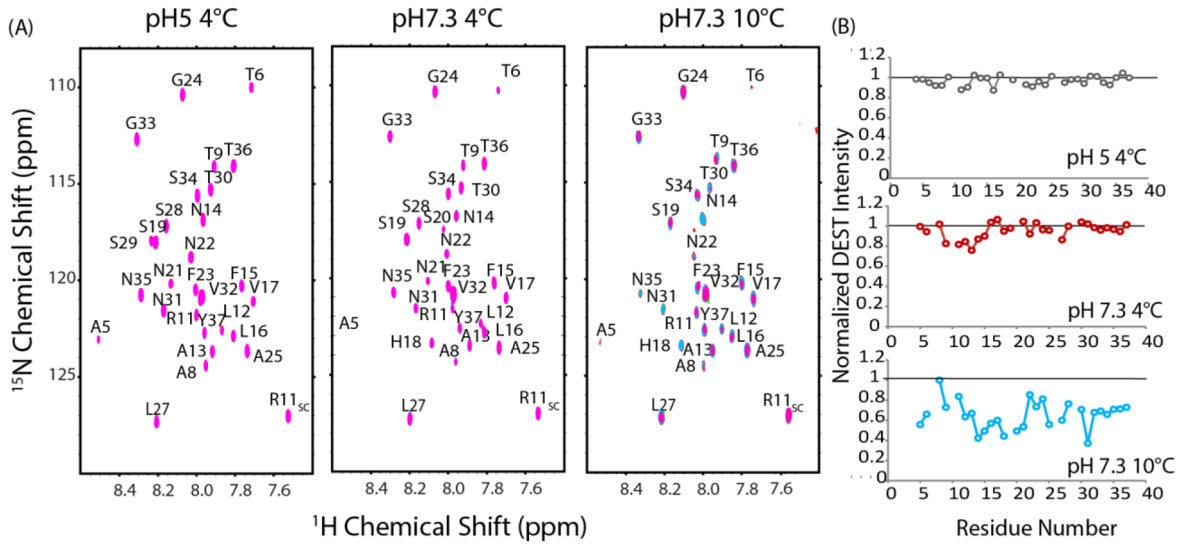

Figure 9. Changes in self-interaction profile with pH and temperature through DEST NMR experiments. (A) DEST NMR spectra of 78 μM hIAPP free acid at pH 5 and 4 °C, pH 7.3 and 4 °C, and pH 7.3 and 10 °C in a solution of 20 mM phosphate buffer and 50 mM NaCl. Pink contours represent saturation at 30 kHz off-resonance; blue contours are from 5 kHz off-resonance saturation. (B) Changes in relative intensity upon saturation expressed as the ratio between the intensity at 5 and 30 kHz off-resonance saturation.

spectrum caused by the association of the monomer with the oligomer is used as a probe to detect self-association sites within the hIAPP peptide. A weak RF field is applied far off-resonance to saturate the underlying but invisible oligomer states. The bound monomer has a significantly higher transverse relaxation rate (R_2) than the free monomer because of the longer rotational correlation time among other factors, which is reflected in a broader line width and a decrease in intensity when it dissociates from the oligomer. This increase in R_2 is residue-specific; residues which are not in contact with the oligomer and do not have their motion restricted by binding have smaller changes in R_2. Considering that a large number of possible bound conformations exist, the magnitude of the changes in R_2 therefore report the fraction of conformations in which that residue is bound.[62] As a consequence, larger decreases in intensity upon saturation in the DEST experiment reflect regions of the hIAPP monomer having stronger contacts with the hIAPP oligomer.

In the original DEST experiment performed on a Aβ monomer protofibril system, the RF offset was varied to solve the full McConnell relaxation equations to get not only changes in R_2 but also the kinetic constants related to the equilibria.[62] Unfortunately, hIAPP is considerably less stable then Aβ, and it was impossible to collect enough points to solve the McConnell relaxation equations before the effects of aggregation became apparent. Instead, the data was interpreted semiquantitatively using the decrease in intensity at given offsets due to the saturation of the underlying invisible oligomer state.

Notwithstanding, clear trends emerged with the DEST-like experiment as a function of temperature and pH. At pH 5 and 4 °C where aggregation is slowest and both the pyrene (Figure 6) and NMR experiments (Figure 5B,C) fail to detect oligomers, no decrease in intensity was detected for any residue in the DEST profile (Figure 9A left and 9B top). The DEST experiment at low pH below the critical temperature therefore serves as a negative control to confirm that intensity changes upon saturation are not present in the absence of oligomers in the DEST experiment.

The DEST profile changes when the experiment is performed at pH 7.3 but below the critical temperature (4°). Under this condition, micellelike oligomers were not detected by the pyrene (Figure 4) or the NMR experiments (Figure 5). However, the AFM experiments suggest that a separate type of oligomer, substantially smaller than the micellelike oligomer, may exist (Figure 8A). The intensities of resonances corresponding to residues in the N-terminal region of the peptide (residues 9−15) decrease moderately upon off-resonance saturation, while the C-terminus and middle regions of the peptide (residues 16−37) show almost no change (Figure 9A middle and 9B middle). Overall, the data support primarily N-terminal association at low temperatures with minimal involvement of the C-terminus.

A substantially different pattern was obtained near the critical temperature (10 °C). First, the overall intensity of all resonances is greatly reduced upon off-resonance excitation with effects seen further off-resonance than at 4 °C. The decrease in overall intensity indicates that stronger self-association occurs at 10 °C than at 4 °C, in agreement with the pyrene, NMR, and AFM experiments. Unfortunately, the decrease in intensity with the increase in temperature makes certain resonances undetectable, and complications begin to arise from aggregation during the experiment. Nevertheless, although the pattern is not as clear as it is at 4 °C, the self-association appears to be centered at a different set of residues at 10 °C than at 4 °C with residues 12−21 decreasing more than other residues after off-resonance saturation (Figure 9B bottom). In the C-terminus, most of the residues are only moderately affected, with the notable exceptions of N31 and A25-L27, which is a region known to be important for fibrillogenesis[70] and is involved in the early formation of transient β-sheet oligomers.[71] This pattern suggests a shift from the N-terminal contacts observed at 4 °C (primarily residues 9−15) toward interactions closer to the center of the peptide (primarily residues 12−21) as the sample is heated to near the critical temperature needed for micellelike oligomer formation.

DOI: 10.1021/jp511758w
J. Phys. Chem. B XXXX, XXX, XXX−XXX

DISCUSSION

We have shown here that the hIAPP amyloid protein, a model for other unstructured amyloid proteins in many (but not all) respects (1) reversibly forms micellelike aggregates in a manner sharply dependent on hIAPP concentration and temperature, (2) rapidly forms fibers above the concentration needed for the formation of micellelike oligomers and more slowly below it, and (3) shows a different self-association pattern at the atomic level in the early stages of aggregation when micellelike oligomers are present. Micelle formation has previously been proposed to be an off-pathway intermediate for hIAPP based on the apparent concentration independence of aggregation.[41,43,44] While a detailed quantitative understanding still awaits further experimental verification in light of the many kinetic variables involved, our results suggest a more complicated picture with at least two separate mechanisms for nucleation: a less-efficient process occurring within small oligomers dominated by N-terminal self-association and a more efficient process initiated within micellelike oligomers involving more extensive contacts throughout the peptide.

Differences between IAPP Micelles and Detergent-like Micelles. Although the micellelike hIAPP oligomers described above share many properties in common with traditional micelles, it is important to recognize several differences between them and simple spherical micelles such as those formed by detergents. For example, in a detergent micelle system the concentration of monomers above the CMC is typically close to the CMC value.[48] Theoretically, this relationship arises from the strong cooperativity assembly of detergent micelles and the packing restrictions present within the micelle, which limit the micelle size to specific limits (<∼100 molecules).[48] Although the actual concentration of hIAPP monomers is difficult to obtain, a quick comparison of the ^{1}H NMR spectra above and below the critical concentration (Figure 7A) suggests that there is substantially more monomer (or other low-molecular-weight species that can be detected by NMR) than would be expected to exist in a simple micelle model. Instead, the hIAPP oligomers appear to share many properties with mesoscopic clusters, which are large (>50 nm), dynamic, and metastable aggregates formed by the partial phase separation of long-lived smaller complexes from protein monomers in solution.[72] Unlike detergent-like micelles, mesoscopic clusters typically contain only a small fraction of the available protein in solution.[72] It is interesting that mesoscopic clusters also exhibit Ostwald ripening,[73] a process in which larger clusters grow at the expense of smaller ones as time progresses by a desorption−condensation process.[74] Since the stability of amyloid fibers is strongly length-dependent,[75] it is possible that such Ostwald ripening can play a role in the initiation of amyloid assembly if larger clusters favor the creation of longer and therefore more stable nuclei. The disappearance of the smaller oligomers upon the creation of the larger micellelike oligomers (Figures 7 and 8) is suggestive, but by no means conclusive, of such a mechanism.

Micellelike Oligomer Formation May Be a General Phenomenon for Natively Unstructured Amyloidogenic Proteins. Although all experiments in this study were performed on IAPP, it is likely that other amyloidogenic proteins, particularly those which are natively unfolded in the monomeric state,[27] also form protein micelles under specific conditions. Amyloid-beta (Aβ) is probably the most intensively studied amyloidogenic protein because of its potential link to Alzheimer's disease. A variety of techniques have shown that Aβ_{1-40} has a similar monomer/micelle transition to that of IAPP. Pyrene and surface tension studies revealed that micellelike oligomers form Aβ_{1-40} at a critical concentration of 17 μM, which, if formed, causes a sharp increase in the rate of aggregation.[40] Similar studies performed under different conditions have shown variable values for the critical concentration of Aβ_{1-40} of 25 μM (0.1 M Tris, pH 7.4 20 °C)[76] and 8 μM (10 mM phosphate buffer, pH is 7.3, 8 μM),[77] illustrating the role environmental factors may play. Notably the correlation between amyloidogenicity and the critical concentration seems to hold even for the dissimilar Aβ and hIAPP sequences; Aβ has a higher critical concentration and greatly slowed aggregation compared to those of hIAPP under the same conditions.[78,79] Micelles of Aβ_{1-40} have also been directly detected by small-angle neutron scattering.[39] The SANS experiment shows spherocylindrical structures with a radius of 2.4 nm and a length of 11 nm at 4 °C and 100 mM DCl (pH 1).[39] To the best of our knowledge, a critical temperature has not been detected for Aβ_{1-40},[80] although the sensitivity of aggregation to environmental conditions does not mean that such a critical temperature does not exist, at least under some conditions.

Although the evidence is most clear for Aβ and IAPP, some indirect evidence also exists for micelle formation for other natively unfolded amyloidogenic proteins. Calcitonin, for example, shows the characteristic oligomer peak in its NMR spectra at 1000 μM but not at 400 μM at pH 2, indicating a possible micellelike transition in this range.[57] Transferred NOEs from the oligomer to monomer allowed a partial reconstruction of the oligomeric structure, which has a turn structure not present in the monomer.[57] Interestingly, EGCG was shown to completely abolish the formation of the calcitonin oligomer.[57] This observation suggests micellelike oligomers may be targeted by aggregation inhibitors either to shift the critical concentration for oligomer formation or to abolish it completely.

Implications of Critical Concentrations in Experimental Design. The CMCs for both hIAPP and Aβ lie in the low micromolar range where many biochemical experiments are performed, which may lead to apparently conflicting interpretations depending on the concentration used. For example, an increase in concentration from 15 to 20 μM leads to a 33% reduction in $t_{1/2}$. By contrast, a much larger increase from 2 to 10 μM results in an essentially negligible change. Because the critical concentration may be influenced by environmental factors, as seen here by changes in pH, changes in environmental conditions may lead to large changes in rate if the critical concentration is crossed. For example, IAPP[81] and other natively unfolded amyloidogenic proteins[20,21,56,82] frequently have a surprisingly large sensitivity to changes in buffer, with the rate usually scaling with the activity of ions within the Hofmeister series. Buffer sensitivity makes sense in light of the role interfacial tension plays in determining the stability of a micellelike oligomer. Notably, Hofmeister water structure making/breaking effects appear to play a smaller role in IAPP at pH 5.5 where micellelike oligomers could not be detected in our experiments.[81]

Some of the reported variability in the aggregation of these proteins may actually be a result of a switching of the mechanism as a result of crossing the critical points involved in concentration. The mechanism of hIAPP aggregation specifically has been a source of controversy. Real-time NMR

DOI: 10.1021/jp511758w
J. Phys. Chem. B XXXX, XXX, XXX−XXX

experiments of hIAPP at pH 6 and 4 °C by Mishra et al. have shown that the peaks for individual residues do not disappear uniformly as aggregation progresses.[83] Instead, the N-terminal cross-peaks disappear before the C-terminal cross-peaks, implying that the formation of large aggregates that are invisible to NMR begins with the formation of N-terminal contacts,[83] matching well with several other studies showing hIAPP self-association within the N-terminal region.[84]

On the other hand, a parallel 2D-FTIR study at higher temperature and neutral pH suggests that β-sheet formation under these conditions begins in the central region of the peptide rather than the N-terminus, implying that amyloid assembly by IAPP under these conditions is distinctly different than amyloid assembly at low pH and lower temperatures.[85] The DEST experiment shows that these apparent discrepancies may reflect the existence of different oligomers above and below the critical temperature. Below the critical temperature, we see limited association entirely within the N-terminal region, as was observed in Mishra's et al.'s NMR experiments.[83] Above the critical temperature, the DEST interaction profile indicates a much more prominent role for self-association in the central region, in agreement with the 2D-FTIR study. A third mechanism involving initial oligomer formation by the interaction of H18 with the C-terminus has been reported at pH 6 and 25 °C,[30] indicating that there may be regions in the phase diagram of hIAPP that remain to be explored. Although pyrene fluorescence holds potential for screening purposes, there is significant room for improvement in the design of chemical probe for micellelike and other types of oligomers. In particular, pyrene has very low solubility, which limits many types of binding studies, and the UV-detected fluorescence is not easy to adapt to a microplate format. The development of a more soluble fluorophore with excitation in the visible range would allow high-throughput screening to map the phase diagram of hIAPP aggregation more completely.

A similar switch in mechanism with concentration has also been observed with Aβ_{1-42}. In a narrow concentration range (20−25 μM), globular Aβ_{1-42} oligomers formed that were positive for the oligomer-specific A11 antibody and showed a high capacity to disrupt lipid bilayers.[86] By contrast, at higher concentrations a different type of oligomer was formed that did not react with the A11 antibody that did not disrupt lipid bilayers, despite having a similar size and secondary structure at low concentrations (<20 μM).[86] Studies such as these show the importance of recognizing the influence of concentration-dependent mechanistic changes and the need for accurate concentration measurements before the start of experiments to minimize batch-to-batch variation and apparent irreproducibility. In this context, it is important to note that some commercial preparations of amyloidogenic peptides made by chemical synthesis contain high levels of salt (in some cases, in excess of 50 wt %) that can vary substantially from lot to lot.

Although many biochemical experiments are performed in the micromolar range, the physiological concentration of most amyloidogenic proteins is much lower, usually in the pico- to nanomolar range.[87,88] This concentration range has been largely unexplored, with the exception of several single-molecule studies[89−92] and a few other types of studies.[25] However, while the circulating concentrations of amyloid peptides are frequently very low, transient concentrations can be quite high in some situations. For example, extracellular Aβ may be internalized by endocytosis or phagocytosis and trafficked to multivesicular bodies.[93] Within these bodies, Aβ can reach a concentration 2 orders of magnitude higher than the circulating concentration.[87]

There are several reasons to believe the critical concentration phenomenon may be relevant to aggregation for IAPP under physiological conditions. First, the critical concentration of hIAPP (the naturally occurring form) is very low (~2 μM for the naturally occurring amidated form, Figure 1). Second, hIAPP is initially stored at millimolar local concentrations in a stable form at low pH[94] before being diluted to picomolar levels in the bloodstream.[95] This is far in excess of the critical concentration for oligomer formation reported here and suggests that IAPP undergoes at least one passage through the critical concentration before dilution in the bloodstream. Critical concentration phenomenoma may also be important in vivo for other amyloidogenic proteins that occur at high concentrations such as SEVI.[96]

■ ASSOCIATED CONTENT

Supporting Information

Materials and methods, time courses for the thioflavin T experiment, log−log transform of the $t_{1/2}$ values from the thioflavin T experiment, and ^{15}N SOFAST-HMQC spectra of hIAPP free acid after a return to 4° after the temperature jump. This material is available free of charge via the Internet at http://pubs.acs.org.

■ AUTHOR INFORMATION

Corresponding Author

*Phone: +1 734 647-6572. E-mail: ramamoor@umich.edu.

Author Contributions

J.R.B., J.K., and M.F.M.S. contributed equally to this work.

Notes

The authors declare no competing financial interest.

■ ACKNOWLEDGMENTS

We thank Dr. Nicholas Fawzi for assistance with the DEST-like experiments. This study was supported by funds from the NIH (GM084018 and GM095640 to A.R.).

■ REFERENCES

(1) Ross, C. A.; Poirier, M. A. Protein Aggregation and Neurodegenerative Disease. *Nat. Med.* **2004**, *10*, S10−S17.

(2) Harrison, R. S.; Sharpe, P. C.; Singh, Y.; Fairlie, D. P. Amyloid Peptides and Proteins in Review. *Rev. Physiol. Biochem. Pharm.* **2007**, *159*, 1−77.

(3) Hamley, I. W. The Amyloid Beta Peptide: A Chemist's Perspective. Role in Alzheimer's and Fibrillization. *Chem. Rev.* **2012**, *112*, 5147−5192.

(4) Marchesi, V. T. Alzheimer's Disease 2012: The Great Amyloid Gamble. *Am. J. Pathol.* **2012**, *180*, 1762−1767.

(5) Liu, T. Y.; Bitan, G. Modulating Self-Assembly of Amyloidogenic Proteins as a Therapeutic Approach for Neurodegenerative Diseases: Strategies and Mechanisms. *ChemMedChem.* **2012**, *7*, 359−374.

(6) Hortschansky, P.; Schroeckh, V.; Christopeit, T.; Zandomeneghi, G.; Fandrich, M. The Aggregation Kinetics of Alzheimer's Beta-Amyloid Peptide Is Controlled by Stochastic Nucleation. *Protein Sci.* **2005**, *14*, 1753−1759.

(7) Giehm, L.; Otzen, D. E. Strategies to Increase the Reproducibility of Protein Fibrillization in Plate Reader Assays. *Anal. Biochem.* **2010**, *400*, 270−281.

(8) Teplow, D. B. On the Subject of Rigor in the Study of Amyloid Beta-Protein Assembly. *Alzheimer's Res. Ther.* **2013**, *5*, 39.

(9) Veeraraghavalu, K.; Zhang, C.; Miller, S.; Hefendehl, J. K.; Rajapaksha, T. W.; Ulrich, J.; Jucker, M.; Holtzman, D. M.; Tanzi, R.

DOI: 10.1021/jp511758w
J. Phys. Chem. B XXXX, XXX, XXX−XXX

E.; Vassar, R.; et al. Comment on "ApoE-Directed Therapeutics Rapidly Clear Beta-Amyloid and Reverse Deficits in AD Mouse Models". *Science* **2013**, *340*, 924.
(10) Tesseur, I.; Lo, A. C.; Roberfroid, A.; Dietvorst, S.; Van Broeck, B.; Borgers, M.; Gijsen, H.; Moechars, D.; Mercken, M.; Kemp, J.; et al. Comment on "ApoE-Directed Therapeutics Rapidly Clear Beta-Amyloid and Reverse Deficits in AD Mouse Models". *Science* **2013**, *340*, 924.
(11) Landreth, G. E.; Cramer, P. E.; Lakner, M. M.; Cirrito, J. R.; Wesson, D. W.; Brunden, K. R.; Wilson, D. A. Response to Comments on "ApoE-Directed Therapeutics Rapidly Clear Beta-Amyloid and Reverse Deficits in Ad Mouse Models". *Science* **2013**, *340*, 924.
(12) Price, A. R.; Xu, G. L.; Siemienski, Z. B.; Smithson, L. A.; Borchelt, D. R.; Golde, T. E.; Felsenstein, K. M. Comment on "ApoE-Directed Therapeutics Rapidly Clear Beta-Amyloid and Reverse Deficits in AD Mouse Models". *Science* **2013**, *340*, 924.
(13) Fitz, N. F.; Cronican, A. A.; Lefterov, I.; Koldamova, R. Comment on "ApoE-Directed Therapeutics Rapidly Clear Beta-Amyloid and Reverse Deficits in AD Mouse Models". *Science* **2013**, *340*, 924.
(14) Cramer, P. E.; Cirrito, J. R.; Wesson, D. W.; Lee, C. Y. D.; Karlo, J. C.; Zinn, A. E.; Casali, B. T.; Restivo, J. L.; Goebel, W. D.; James, M. J.; et al. ApoE-Directed Therapeutics Rapidly Clear Beta-Amyloid and Reverse Deficits in AD Mouse Models. *Science* **2012**, *335*, 1503−1506.
(15) Pimplikar, S. W. Reassessing the Amyloid Cascade Hypothesis of Alzheimer's Disease. *Int. J. Biochem. Cell B* **2009**, *41*, 1261−1268.
(16) Benilova, I.; Karran, E.; De Strooper, B. The Toxic Aβ Oligomer and Alzheimer's Disease: An Emperor in Need of Clothes. *Nat. Neurosci.* **2012**, *15*, 349−357.
(17) Haataja, L.; Gurlo, T.; Huang, C. J.; Butler, P. C. Islet Amyloid in Type 2 Diabetes, and the Toxic Oligomer Hypothesis. *Endocr. Rev.* **2008**, *29*, 303−316.
(18) Fandrich, M. Oligomeric Intermediates in Amyloid Formation: Structure Determination and Mechanisms of Toxicity. *J. Mol. Biol.* **2012**, *421*, 427−440.
(19) Haass, C.; Selkoe, D. J. Soluble Protein Oligomers in Neurodegeneration: Lessons from the Alzheimer's Amyloid Beta-Peptide. *Nat. .Rev. Mol. Cell. Biol.* **2007**, *8*, 101−112.
(20) Garvey, M.; Tepper, K.; Haupt, C.; Knupfer, U.; Klement, K.; Meinhardt, J.; Horn, U.; Balbach, J.; Fandrich, M. Phosphate and HEPES Buffers Potently Affect the Fibrillation and Oligomerization Mechanism of Alzheimer's Aβ Peptide. *Biochem. Biophys. Res. Commun.* **2011**, *409*, 385−388.
(21) Olsen, J. S.; DiMaio, J. T. M.; Doran, T. M.; Brown, C.; Nilsson, B. L.; Dewhurst, S. Seminal Plasma Accelerates Semen-Derived Enhancer of Viral Infection (SEVI) Fibril Formation by the Prostatic Acid Phosphatase (Pap(248−286)) Peptide. *J. Biol. Chem.* **2012**, *287*, 11842−11849.
(22) Pronchik, J.; He, X. L.; Giurleo, J. T.; Talaga, D. S. In Vitro Formation of Amyloid from Alpha-Synuclein Is Dominated by Reactions at Hydrophobic Interfaces. *J. Am. Chem. Soc.* **2010**, *132*, 9797−9803.
(23) Teplow, D. B. Preparation of Amyloid Beta-Protein for Structural and Functional Studies. *Methods Enzymol.* **2006**, *413*, 20−33.
(24) Stine, W. B.; Jungbauer, L.; Yu, C. J.; Ladu, M. J. Preparing Synthetic a Beta in Different Aggregation States. *Methods Mol. Biol.* **2011**, *670*, 13−32.
(25) Hellstrand, E.; Boland, B.; Walsh, D. M.; Linse, S. Amyloid Beta-Protein Aggregation Produces Highly Reproducible Kinetic Data and Occurs by a Two-Phase Process. *ACS Chem. Neurosci.* **2010**, *1*, 13−18.
(26) Westermark, P.; Andersson, A.; Westermark, G. T. Islet Amyloid Polypeptide, Islet Amyloid, and Diabetes Mellitus. *Physiol Rev.* **2011**, *91*, 795−826.
(27) Uversky, V. N.; Fink, A. L. Conformational Constraints for Amyloid Fibrillation: The Importance of Being Unfolded. *Biochim. Biophys. Acta* **2004**, *1698*, 131−153.
(28) Yonemoto, I. T.; Kroon, G. J.; Dyson, H. J.; Balch, W. E.; Kelly, J. W. Amylin Proprotein Processing Generates Progressively More Amyloidogenic Peptides That Initially Sample the Helical State. *Biochemistry* **2008**, *47*, 9900−9910.
(29) Tu, L.-H.; Serrano, A. L.; Zanni, M. T.; Raleigh, D. P. Mutational Analysis of Preamyloid Intermediates: The Role of His-Tyr Interactions in Islet Amyloid Formation. *Biophys. J.* **2014**, *106*, 1520−1527.
(30) Wei, L.; Jiang, P.; Xu, W. X.; Li, H.; Zhang, H.; Yan, L. Y.; Chan-Park, M. B.; Liu, X. W.; Tang, K.; Mu, Y. G.; et al. The Molecular Basis of Distinct Aggregation Pathways of Islet Amyloid Polypeptide. *J. Biol. Chem.* **2011**, *286*, 6291−6300.
(31) Padrick, S. B.; Miranker, A. D. Islet Amyloid Polypeptide: Identification of Long-Range Contacts and Local Order on the Fibrillogenesis Pathway. *J. Mol. Biol.* **2001**, *308*, 783−794.
(32) Nanga, R. P. R.; Brender, J. R.; Vivekanandan, S.; Ramamoorthy, A. Structure and Membrane Orientation of IAPP in Its Natively Amidated Form at Physiological pH in a Membrane Environment. *Biochim. Biophys. Acta* **2011**, *1808*, 2337−2342.
(33) Lomakin, A.; Chung, D. S.; Benedek, G. B.; Kirschner, D. A.; Teplow, D. B. On the Nucleation and Growth of Amyloid Beta-Protein Fibrils: Detection of Nuclei and Quantitation of Rate Constants. *Proc. Natl. Acad. Sci. U.S.A.* **1996**, *93*, 1125−1129.
(34) Lomakin, A.; Teplow, D. B.; Kirschner, D. A.; Benedek, G. B. Kinetic Theory of Fibrillogenesis of Amyloid Beta-Protein. *Proc. Natl. Acad. Sci. U.S.A.* **1997**, *94*, 7942−7947.
(35) Kashchiev, D.; Cabriolu, R.; Auer, S. Confounding the Paradigm: Peculiarities of Amyloid Fibril Nucleation. *J. Am. Chem. Soc.* **2013**, *135*, 1531−1539.
(36) Pellarin, R.; Friedman, R.; Caflisch, A. Amyloid Aggregation on Lipid Bilayers and Its Impact on Membrane Permeability. *J. Mol. Biol.* **2009**, *387*, 407−415.
(37) Oosawa, F.; Asakura, S. *Thermodynamics of the Polymerization of Protein*; Academic Press: London, 1975; pg. 204.
(38) Hong, L.; Qi, X. H.; Zhang, Y. Dissecting the Kinetic Process of Amyloid Fiber Formation through Asymptotic Analysis. *J. Phys. Chem. B* **2012**, *116*, 6611−6617.
(39) Yong, W.; Lomakin, A.; Kirkitadze, M. D.; Teplow, D. B.; Chen, S. H.; Benedek, G. B. Structure Determination of Micelle-Like Intermediates in Amyloid Beta-Protein Fibril Assembly by Using Small Angle Neutron Scattering. *Proc. Natl. Acad. Sci. U.S.A.* **2002**, *99*, 150−154.
(40) Sabate, R.; Estelrich, J. Evidence of the Existence of Micelles in the Fibrillogenesis of Beta-Amyloid Peptide. *J. Phys. Chem. B* **2005**, *109*, 11027−11032.
(41) Rhoades, E.; Gafni, A. Micelle Formation by a Fragment of Human Islet Amyloid Polypeptide. *Biophys. J.* **2003**, *84*, 3480−3487.
(42) Jean, L.; Lee, C. F.; Lee, C.; Shaw, M.; Vaux, D. J. Competing Discrete Interfacial Effects Are Critical for Amyloidogenesis. *FASEB J.* **2010**, *24*, 309−317.
(43) Padrick, S. B.; Miranker, A. D. Islet Amyloid: Phase Partitioning and Secondary Nucleation Are Central to the Mechanism of Fibrillogenesis. *Biochemistry* **2002**, *41*, 4694−4703.
(44) Rhoades, E.; Agarwal, J.; Gafni, A. Aggregation of an Amyloidogenic Fragment of Human Islet Amyloid Polypeptide. *Biochim. Biophys. Acta* **2000**, *1476*, 230−238.
(45) Kalyanasundaram, K.; Thomas, J. K. Environmental Effects on Vibronic Band Intensities in Pyrene Monomer Fluorescence and Their Application in Studies of Micellar Systems. *J. Am. Chem. Soc.* **1977**, *99*, 2039−2044.
(46) Ruiz, C. C.; Aguiar, J.; Carpena, P.; Molina-Bolivar, J. A. On the Determination of the Critical Micelle Concentration by the Pyrene 1:3 Ratio Method. *J. Colloid Interface Sci.* **2003**, *258*, 116−122.
(47) Reinke, A. A.; Ung, P. M. U.; Quintero, J. J.; Carlson, H. A.; Gestwicki, J. E. Chemical Probes That Selectively Recognize the Earliest Aβ Oligomers in Complex Mixtures. *J. Am. Chem. Soc.* **2010**, *132*, 17655−17657.
(48) Israelachvili, J. N. *Intermolecular and Surface Forces*, 3rd ed.; Academic Press: Burlington, MA, 2011; p 674.
(49) Jan, A.; Hartley, D. M.; Lashuel, H. A. Preparation and Characterization of Toxic Aβ Aggregates for Structural and Functional

DOI: 10.1021/jp511758w
J. Phys. Chem. B XXXX, XXX, XXX−XXX

Studies in Alzheimer's Disease Research. *Nat. Protoc.* **2010**, *5*, 1186−1209.
(50) Pan, J.; Han, J.; Borchers, C. H.; Konermann, L. Structure and Dynamics of Small Soluble Aβ(1−40) Oligomers Studied by Top-Down Hydrogen Exchange Mass Spectrometry. *Biochemistry* **2012**, *51*, 3694−3703.
(51) Woodbury, R. L.; Hardy, S. J.; Randall, L. L. Complex Behavior in Solution of Homodimeric Seca. *Protein Sci.* **2002**, *11*, 875−882.
(52) Barbar, E. NMR Characterization of Partially Folded and Unfolded Conformational Ensembles of Proteins. *Biopolymers* **1999**, *51*, 191−207.
(53) Brender, J. R.; Hartman, K.; Reid, K. R.; Kennedy, R. T.; Ramamoorthy, A. A Single Mutation in the Nonamyloidogenic Region of Islet Amyloid Polypeptide Greatly Reduces Toxicity. *Biochemistry* **2008**, *47*, 12680−12688.
(54) Cao, P.; Abedini, A.; Wang, H.; Tu, L. H.; Zhang, X.; Schmidt, A. M.; Raleigh, D. P. Islet Amyloid Polypeptide Toxicity and Membrane Interactions. *Proc. Natl. Acad. Sci. U.S.A.* **2013**, *110*, 19279−19284.
(55) Radovan, D.; Smirnovas, V.; Winter, R. Effect of Pressure on Islet Amyloid Polypeptide Aggregation: Revealing the Polymorphic Nature of the Fibrillation Process. *Biochemistry* **2008**, *47*, 6352−6360.
(56) Narayanan, S.; Reif, B. Characterization of Chemical Exchange between Soluble and Aggregated States of Beta-Amyloid by Solution-State NMR Upon Variation of Salt Conditions. *Biochemistry* **2005**, *44*, 1444−1452.
(57) Huang, R.; Vivekanandan, S.; Brender, J. R.; Abe, Y.; Naito, A.; Ramamoorthy, A. NMR Characterization of Monomeric and Oligomeric Conformations of Human Calcitonin and Its Interaction with EGCG. *J. Mol. Biol.* **2012**, *416*, 108−120.
(58) Krishnamoorthy, J.; Brender, J. R.; Vivekanandan, S.; Jahr, N.; Ramamoorthy, A. Side-Chain Dynamics Reveals Transient Association of Aβ(1−40) Monomers with Amyloid Fibers. *J. Phys. Chem. B* **2012**, *116*, 13618−13623.
(59) Dorgeret, B.; Khemtemourian, L.; Correia, I.; Soulier, J. L.; Lequin, O.; Ongeri, S. Sugar-Based Peptidomimetics Inhibit Amyloid Beta-Peptide Aggregation. *Eur. J. Med. Chem.* **2011**, *46*, 5959−5969.
(60) Soong, R.; Brender, J. R.; Macdonald, P. M.; Ramamoorthy, A. Association of Highly Compact Type Ii Diabetes Related Islet Amyloid Polypeptide Intermediate Species at Physiological Temperature Revealed by Diffusion NMR Spectroscopy. *J. Am. Chem. Soc.* **2009**, *131*, 7079−7085.
(61) Fawzi, N. L.; Ying, J.; Torchia, D. A.; Clore, G. M. Kinetics of Amyloid Beta Monomer-to-Oligomer Exchange by Nmr Relaxation. *J. Am. Chem. Soc.* **2010**, *132*, 9948−9951.
(62) Fawzi, N. L.; Ying, J. F.; Ghirlando, R.; Torchia, D. A.; Clore, G. M. Atomic-Resolution Dynamics on the Surface of Amyloid-Beta Protofibrils Probed by Solution NMR. *Nature* **2011**, *480*, 268−272.
(63) Fawzi, N. L.; Ying, J. F.; Torchia, D. A.; Clore, G. M. Probing Exchange Kinetics and Atomic Resolution Dynamics in High-Molecular-Weight Complexes Using Dark-State Exchange Saturation Transfer Nmr Spectroscopy. *Nat. Protoc.* **2012**, *7*, 1523−1533.
(64) Esposito, V.; Das, R.; Melacini, G. Mapping Polypeptide Self-Recognition through H-1 Off-Resonance Relaxation. *J. Am. Chem. Soc.* **2005**, *127*, 9358−9359.
(65) Algamal, M.; Milojevic, J.; Jafari, N.; Zhang, W.; Melacini, G. Mapping the Interactions between the Alzheimer's Abeta-Peptide and Human Serum Albumin Beyond Domain Resolution. *Biophys. J.* **2013**, *105*, 1700−1709.
(66) Milojevic, J.; Costa, M.; Ortiz, A. M.; Jorquera, J. I.; Melacini, G. In Vitro Amyloid-Beta Binding and Inhibition of Amyloid-Beta Self-Association by Therapeutic Albumin. *J. Alzheimer's Dis.* **2014**, *38*, 753−765.
(67) Milojevic, J.; Melacini, G. Stoichiometry and Affinity of the Human Serum Albumin-Alzheimer's Abeta Peptide Interactions. *Biophys. J.* **2011**, *100*, 183−92.
(68) Milojevic, J.; Raditsis, A.; Melacini, G. Human Serum Albumin Inhibits Abeta Fibrillization through a "Monomer-Competitor" Mechanism. *Biophys. J.* **2009**, *97*, 2585−2594.
(69) Raditsis, A. V.; Milojevic, J.; Melacini, G. Aβ Association Inhibition by Transferrin. *Biophys. J.* **2013**, *105*, 473−480.
(70) Abedini, A.; Meng, F. L.; Raleigh, D. P. A Single-Point Mutation Converts the Highly Amyloidogenic Human Islet Amyloid Polypeptide into a Potent Fibrillization Inhibitor. *J. Am. Chem. Soc.* **2007**, *129*, 11300−11301.
(71) Buchanan, L. E.; Dunkelberger, E. B.; Tran, H. Q.; Cheng, P. N.; Chiu, C. C.; Cao, P.; Raleigh, D. P.; de Pablo, J. J.; Nowick, J. S.; Zanni, M. T. Mechanism of IAPP Amyloid Fibril Formation Involves an Intermediate with a Transient Beta-Sheet. *Proc. Natl. Acad. Sci. U.S.A.* **2013**, *110*, 19285−19290.
(72) Pan, W.; Vekilov, P. G.; Lubchenko, V. Origin of Anomalous Mesoscopic Phases in Protein Solutions. *J. Phys. Chem. B* **2010**, *114*, 7620−7630.
(73) Li, Y.; Lubchenko, V.; Vorontsova, M. A.; Filobelo, L.; Vekilov, P. G. Ostwald-Like Ripening of the Anomalous Mesoscopic Clusters in Protein Solutions. *J. Phys. Chem. B* **2012**, *116*, 10657−10664.
(74) Lifshitz, I. M.; Slyozov, V. V. The Kinetics of Precipitation from Supersaturated Solid Solutions. *J. Phys. Chem. Solids* **1961**, *19*, 35−50.
(75) Linse, B.; Linse, S. Monte Carlo Simulations of Protein Amyloid Formation Reveal Origin of Sigmoidal Aggregation Kinetics. *Mol. Biosyst.* **2011**, *7*, 2296−2303.
(76) Soreghan, B.; Kosmoski, J.; Glabe, C. Surfactant Properties of Alzheimer's a Beta Peptides and the Mechanism of Amyloid Aggregation. *J. Biol. Chem.* **1994**, *269*, 28551−28554.
(77) Lei, L. Z. Ph.D. Thesis. *Mechanism of Early Stage Abeta Amyloid Formation*. Case Western Reserve University, 2008.
(78) Suzuki, Y.; Brender, J. R.; Hartman, K.; Ramamoorthy, A.; Marsh, E. N. G. Alternative Pathways of Human Islet Amyloid Polypeptide Aggregation Distinguished by F-19 Nuclear Magnetic Resonance-Detected Kinetics of Monomer Consumption. *Biochemistry* **2012**, *51*, 8154−8162.
(79) Suzuki, Y.; Brender, J. R.; Soper, M. T.; Krishnamoorthy, J.; Zhou, Y. L.; Ruotolo, B. T.; Kotov, N. A.; Ramamoorthy, A.; Marsh, E. N. G. Resolution of Oligomeric Species During the Aggregation of Aβ(1−40) Using F-19 NMR. *Biochemistry* **2013**, *52*, 1903−1912.
(80) Kusumoto, Y.; Lomakin, A.; Teplow, D. B.; Benedek, G. B. Temperature Dependence of Amyloid Beta-Protein Fibrillization. *Proc. Natl. Acad. Sci. U.S.A.* **1998**, *95*, 12277−12282.
(81) Marek, P. J.; Patsalo, V.; Green, D. F.; Raleigh, D. P. Ionic Strength Effects on Amyloid Formation by Amylin Are a Complicated Interplay among Debye Screening, Ion Selectivity, and Hofmeister Effects. *Biochemistry* **2012**, *51*, 8478−8490.
(82) Yeh, V.; Broering, J. M.; Romanyuk, A.; Chen, B.; Chernoff, Y. O.; Bommarius, A. S. The Hofmeister Effect on Amyloid Formation Using Yeast Prion Protein. *Protein Sci.* **2010**, *19*, 47−56.
(83) Mishra, R.; Geyer, M.; Winter, R. Nmr Spectroscopic Investigation of Early Events in IAPP Amyloid Fibril Formation. *ChemBioChem* **2009**, *10*, 1769−72.
(84) Mazor, Y.; Gilead, S.; Benhar, I.; Gazit, E. Identification and Characterization of a Novel Molecular-Recognition and Self-Assembly Domain within the Islet Amyloid Polypeptide. *J. Mol. . Biol.* **2002**, *322*, 1013−1024.
(85) Shim, S. H.; Gupta, R.; Ling, Y. L.; Strasfeld, D. B.; Raleigh, D. P.; Zanni, M. T. Two-Dimensional IR Spectroscopy and Isotope Labeling Defines the Pathway of Amyloid Formation with Residue-Specific Resolution. *Proc. Natl. Acad. Sci. U.S.A.* **2009**, *106*, 6614−6619.
(86) Ladiwala, A. R. A.; Litt, J.; Kane, R. S.; Aucoin, D. S.; Smith, S. O.; Ranjan, S.; Davis, J.; Van Nostrand, W. E.; Tessier, P. M. Conformational Differences between Two Amyloid Beta Oligomers of Similar Size and Dissimilar Toxicity. *J. Biol. Chem.* **2012**, *287*, 24765−24773.
(87) Hu, X. Y.; Crick, S. L.; Bu, G. J.; Frieden, C.; Pappu, R. V.; Lee, J. M. Amyloid Seeds Formed by Cellular Uptake, Concentration, and Aggregation of the Amyloid-Beta Peptide. *Proc. Natl. Acad. Sci. U.S.A.* **2009**, *106*, 20324−20329.
(88) Kuo, Y. M.; Emmerling, M. R.; Lampert, H. C.; Hempelman, S. R.; Kokjohn, T. A.; Woods, A. S.; Cotter, R. J.; Roher, A. E. High

DOI: 10.1021/jp511758w
J. Phys. Chem. B XXXX, XXX, XXX−XXX

Levels of Circulating Abeta42 Are Sequestered by Plasma Proteins in Alzheimer's Disease. *Biochem. Biophys. Res. Commun.* **1999**, *257*, 787−791.
(89) Ding, H.; Wong, P. T.; Lee, E. L.; Gafni, A.; Steel, D. G. Determination of the Oligomer Size of Amyloidogenic Protein Beta-Amyloid(1−40) by Single-Molecule Spectroscopy. *Biophys. J.* **2009**, *97*, 912−921.
(90) Johnson, R. D.; Schauerte, J. A.; Wisser, K. C.; Gafni, A.; Steel, D. G. Direct Observation of Single Amyloid-Beta(1−40) Oligomers on Live Cells: Binding and Growth at Physiological Concentrations. *PLoS One* **2011**, *6*, e23970.
(91) Sengupta, P.; Garai, K.; Sahoo, B.; Shi, Y.; Callaway, D. J. E.; Maiti, S. The Amyloid Beta Peptide (a Beta(1−40)) Is Thermodynamically Soluble at Physiological Concentrations. *Biochemistry* **2003**, *42*, 10506−10513.
(92) Nag, S.; Sarkar, B.; Bandyopadhyay, A.; Sahoo, B.; Sreenivasan, V. K.; Kombrabail, M.; Muralidharan, C.; Maiti, S. Nature of the Amyloid-Beta Monomer and the Monomer-Oligomer Equilibrium. *J. Biol. Chem.* **2011**, *286*, 13827−33.
(93) Friedrich, R. P.; Tepper, K.; Roznicke, R.; Soom, M.; Westermann, M.; Reymann, K.; Kaether, C.; Fandrich, M. Mechanism of Amyloid Plaque Formation Suggests an Intracellular Basis of Aβ Pathogenicity. *Proc. Natl. Acad. Sci. U.S.A.* **2010**, *107*, 1942−1947.
(94) Knight, J. D.; Williamson, J. A.; Miranker, A. D. Interaction of Membrane-Bound Islet Amyloid Polypeptide with Soluble and Crystalline Insulin. *Protein Sci.* **2008**, *17*, 1850−1856.
(95) Butler, P. C.; Chou, J.; Carter, W. B.; Wang, Y. N.; Bu, B. H.; Chang, D.; Chang, J. K.; Rizza, R. A. Effects of Meal Ingestion on Plasma Amylin Concentration in Niddm and Nondiabetic Humans. *Diabetes* **1990**, *39*, 752−756.
(96) Munch, J.; Rucker, E.; Standker, L.; Adermann, K.; Goffinet, C.; Schindler, M.; Wildum, S.; Chinnadurai, R.; Rajan, D.; Specht, A.; et al. Semen-Derived Amyloid Fibrils Drastically Enhance HIV Infection. *Cell* **2007**, *131*, 1059−1071.

DOI: 10.1021/jp511758w
J. Phys. Chem. B XXXX, XXX, XXX−XXX